DESIGN AND INITIAL RUN OF A NEW TEST SETUP FOR INVESTIGATIONS ON THE AEROELASTIC STABILITY OF PANELS IN THE TRANSONIC MACH DOMAIN

J. Lübker [(1)], M. Alder [(2)], H. Fink [(3)]

[(1)] DLR, German Aerospace Center, Göttingen, 37073, Germany, Jannis.Luebker@DLR.de
[(2)] DLR, German Aerospace Center, Braunschweig, 38108, Germany, Marko.Alder@DLR.de
[(3)] DLR, German Aerospace Center, Göttingen, 37073, Germany, Helena.Fink@DLR.de

ABSTRACT

A flat rectangular plate, clamped on all sides and actuated in its first bending mode, is used for investigations on aeroelastic stability. The described experiment is performed in the Transonic Wind Tunnel Göttingen (DNW-TWG) within a Mach number domain of $0.7 < M_\infty < 1.2$. This forced motion experiment is used for obtaining the aerodynamic response over a wide range of frequencies and amplitudes of the plate's motion. Beside the measurement of the panel deformation by means of a stereo camera marker tracking system, the flow response over the panel is measured by high sensitive miniature pressure transducers. The boundary layer thickness is identified by means of a pitot tube equipped rake. The content of this paper focuses on the design and initial operation of the wind tunnel test setup. In the second part the first results are discussed.

1. INTRODUCTION

Flutter, a dynamic instability, is a phenomenon known for wings as well as for panel structures. Those self-excited instabilities arise from the interaction of aerodynamic loads with the structures elastic and inertial loads. Several experimental approaches were published in the recent decades investigating numerous aspects of panel flutter. The first experimental approach known to the authors was done in 1945 by P. Jordan [1, 2] due to problems occurring at the V2/A4 rocket [3]. The tests were conducted by using panels of different materials, which were subjected to different mechanical boundary conditions. A wide variation of free stream velocities ($70\text{m/s} < c_\infty < 600\text{m/s}$) was considered. Those parameters were getting essential in the panel flutter investigations of the decades to come. During the cold war and the strived predomination in space on both American and Soviet side the interest revived. In the 1960's and 1970's thorough experimental and theoretical research on panel flutter was performed. Many activities were conducted at NASA [4, 5], focusing on rocket technology applications. Muhlstein et al. [6, 7, 8] did extensive investigations on panel flutter in the low supersonic domain ($1.05 < M < 1.4$) by using rectangular plates. His investigations comprised numerous facets, e.g. obtaining flutter boundaries presented by the critical dynamic pressure q_{crit}, which marks the flutter onset. The dynamic pressure is calculated with the fluid density ρ_∞ and the free stream velocity c_∞. The panel stream wise length a and its stiffness D are used for calculating the nondimensional dynamic pressure λ (Eq. 1).

$$\lambda = \frac{\rho_\infty c_\infty^2 a^3}{D} \tag{1}$$

$$D = \frac{E h^3}{12(1-\nu^2)} \tag{2}$$

The panel stiffness (Eq. 2) contains the Young's modulus E and the Poisson number ν. Another nondimensional parameter, analyzed by Muhlstein and Lock et al. [9], was the mass ratio (Eq. 3), which depends on the fluid parameter density ρ_∞ and the structure properties density ρ_s,

streamwise length a and thickness h. They observed that with increasing μ an increase in critical dynamic pressure occurred.

$$\mu = \frac{\rho_\infty a}{\rho_S h} \tag{3}$$

The structure's mechanical boundary conditions (MBC's) have a significant influence on panel flutter. Muhlstein as well as Vedeneev et al. [10] made use of clamped plates on all four edges. Sylvester et al. [11] showed at $M = 1.3$ that panels with four edges clamped are less prone to flutter than panels clamped with only two edges. Muhlstein performed experiments with clamped panels as well. Other activities focused on the influence of streamwise [12] and spanwise [13] curved panels. Furthermore, cavities underneath the panel as well as pressure differences between the flow exposed surface and the back surface were investigated by Muhlstein and Dowell [14]. Pre-stresses due to thermal loads [11] and in-plane loads [16] were examined as well as the influence of CFRP (orthotropic material properties) [17, 18, 19, 20]. Muhlstein's setup provided a change of the panel aspect ratio, which is the panel length a divided by its width w. This change revealed the strong impact of the aspect ratio on the panel flutter boundary and the resulting flutter frequency. Besides those influences, it turned out that the boundary layer may have a significant stabilizing effect on panel flutter in the transonic regime [5]. Several theoretical attempts were made, e.g. the "piston theory" by Ashley [21], approaches based on the unsteady linearized potential flow theory by Dowell [16] and the so called "shear flow" theory by Dowell [16]. All of those theories failed at describing the panel flutter in the transonic regime properly. In the recent years, due to improved computer abilities and enhanced numeric calculation methods, new theoretical approaches were started using coupled finite element methods (FEM) and computational fluid dynamics (CFD) Software. One of those new approaches was done by Hashimoto et al. [22] and shows a better agreement with experimental results mentioned above. The German Aerospace Center (DLR) started an own approach together with Airbus DS to close the gap in simulation capability for the transonic Mach domain and getting a deeper understanding of the physics leading to the phenomenon of panel flutter. On the one hand, those activities comprise numerical investigations, which were recently published by Alder [23] and are based on coupled CFD/CSM calculations. A comparison of the experimental results by Muhlstein et al. with aforesaid theoretical approaches is presented in Fig. 1. Here, the shear flow theory by Dowell [16] shows the largest discrepancy compared to the coupled CFD/FEM approaches. On the other hand, there are experimental activities by means of wind tunnel tests, which are subject of this report. The main focus lies here on the design process of the test setup. Results of the initial run, conducted in winter 2015/2016, are presented as well.

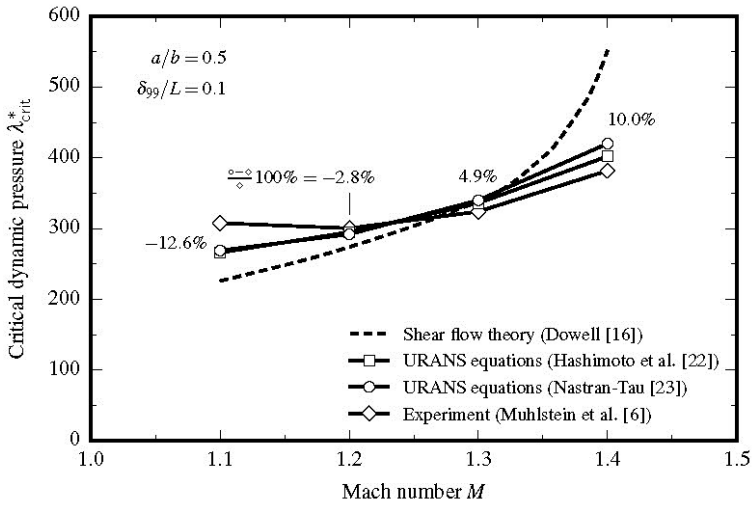

Fig. 1. Experimental results are compared to several theoretical approaches [23].

2. TEST SETUP

Requirements

The test setup used in the presented activities was designed and manufactured to provide a new experimental environment for wind tunnel panel flutter tests at the DLR Institute of Aeroelasticity. Since an investigation of different panels (related to material, size, curvature and mechanical constraints) is intended, the setup had to be designed in a modular fashion. In the first experiments with this setup a model with basic characteristics is to be investigated. The considered parameters are reduced as far as possible to simplify the numerical simulation as well as the analysis of the gained results. The panel consists of a flat plate with clamped mechanical boundary conditions (all six DOF's constraint) for all four edges and is implemented in the wind tunnel's wall. So, only one side of the panel is exposed to the wind tunnel flow. This position was chosen because of the required hydraulic system that will be described later on. Actuators and hydraulic hoses have to be mounted in the vicinity of the panel rear side. With the panel mounted in the middle of the wind tunnel this would have led to an inacceptable blockage in the test section. The occurring of aerodynamic nonlinearities shall be avoided as well.
By conducting a forced motion experiment several aspects important for free flutter experiments can be neglected. The latter demands an exact knowledge about the structure properties for accurate validation calculations. Manufacturing inaccuracies of the panel thickness and of the intended boundary constraints as well as influences of added masses (such as sensors) are to be considered. By forcing the panel into certain motions, by means of an actuator, those structural parameters can be disregarded. With regards to safety precautions free flutter experiments are always associated with the risk of the destruction of the model and damaging the test facility. Controlled oscillations of the test structure and its additional mounting on the actuator rod can remedy the situation. The objective of a forced motion experiment is the investigation of the aerodynamic response to the structure motion. By identifying responses over a certain range of frequencies the transfer function can be determined in this range. The function is only valid for the tested degree of freedom of the system, which means in this case the panel's mode one shape.

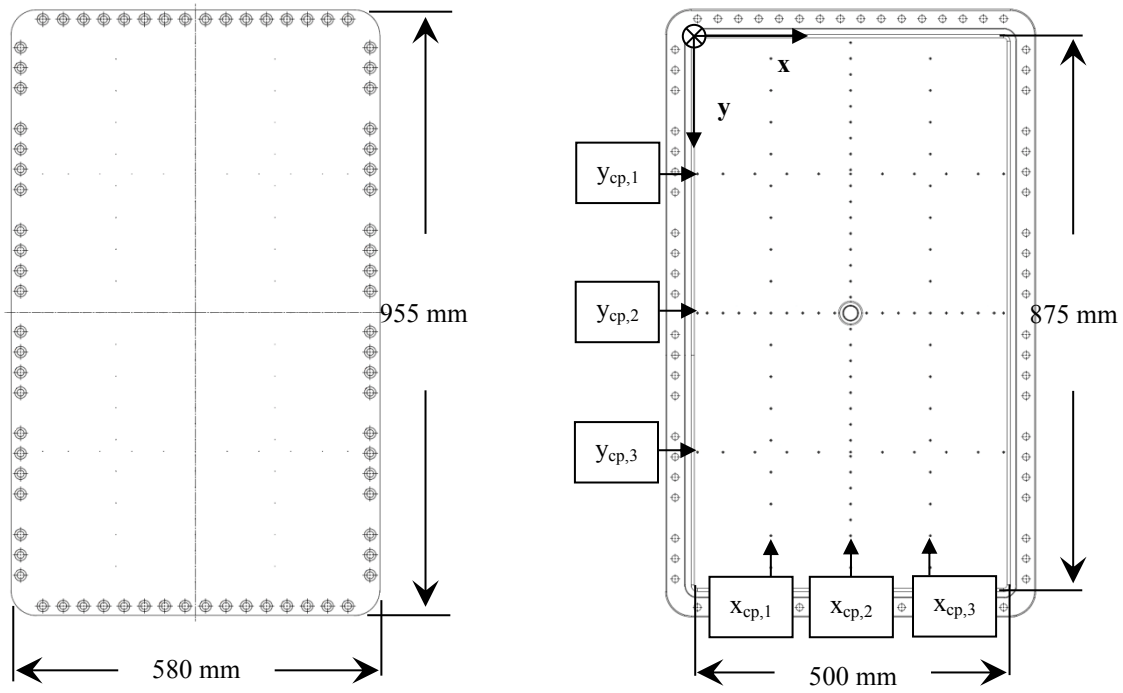

Fig. 2. Top view of the panel (left), rear side of the panel (right). The right part shows the six sections of pressure transducers as well as the panel frame with its bolt connection drill holes and the actuator connection pin in the center.

The second objective is the investigation of energy transfers between flow and structure. For this reason pressure and displacement have to be measured over the panel surface. Measurements of the panel deformation ensure the intended motions and the unsteady pressure probes provide data on the flow response. Owing to the mentioned impact of the turbulent boundary layer a pitot tube wake rake is mounted downstream behind the panel. In the following sections the various parts of the setup will be discussed in more detail.

Panel

A flat plate made of steel of a_o = 550mm by w_o = 925mm outer dimensions outlines the investigated model. The main part of the model is milled out in its center down to a thickness of h_i = 3mm. This area of a_i = 500mm by w_i = 875mm is the actual panel. Due to the milling process a frame structure is shaped at all four edges with h_o = 20mm. This method ensures the intended MBC's (stiffness ratio $D_o/D_i \approx 300$). In addition, the model is bolt mounted on a much stiffer steel framework ($D_3/D_i \approx$ 6200). As the panel will be forced to undergo oscillating motions with different amplitudes steel with a high toughness is chosen (Toolox33). The used coordinate system, depicted in Fig. 2, has its origin at the panel's leading edge.

Forced Motion

Fig. 3. shows the general flutter behavior of a 2D panel in the transonic Mach number domain, which is fixed at leading edge and trailing edge (simply supported). In the low supersonic domain a shape quite similar to the first mode shape is to be expected, so-called single mode flutter. The arising flutter frequency stays in the vicinity of its first natural frequency. Clamped panels show the same behavior regarding flutter shapes and frequencies. In case of 3D panels so-called coupled mode flutter is observed, which means an additional contribution of the second mode shape. With regard to the 2D case results from the panel center lines can be used. For the 3D case a second mode shape has to be realized. In the current setup a hydraulic system is used for moving the panel in the first mode shape. The Hydropuls PLF 7 type hydraulic linear cylinder has a nominal stroke of s = 10.0mm and a nominal force of F = 7kN. The cylinder is controlled by means of an inductive range sensor. Oil pressure of p = 270bar and a flow rate of $\dot{V}$ = 19l/min are necessary for a sound operation of the forced motion test. A rack is mounted behind the panel's back surface and carries the cylinder. The cylinder is then connected to the center of the panel. For that purpose a threaded cone is located there (Fig. 2.).

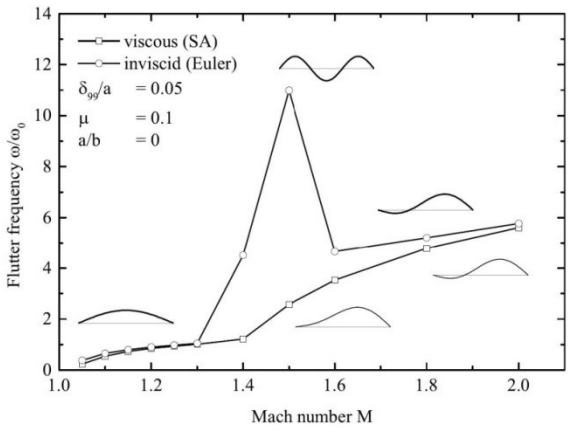

Fig. 3. The flutter frequency plotted against the Mach number. In the transonic domain the system damping becomes negative by oscillating in its first mode shape [22].

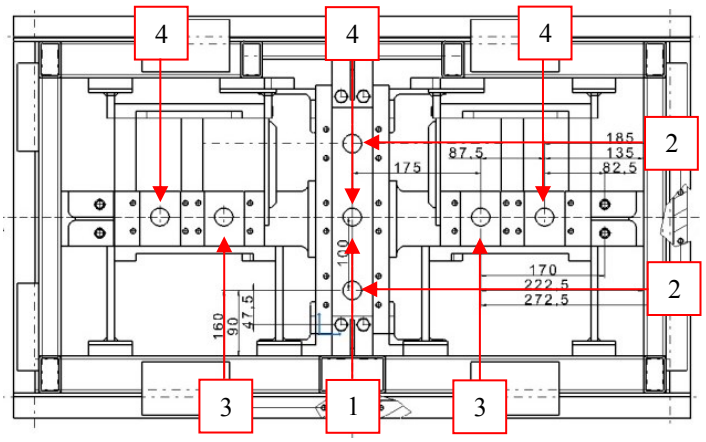

Fig. 4. Top view of the actuator rack. Four different plate mode shapes can be established:
1 → Panel mode 1/1; 2 → Panel mode 2/1;
3 → Panel mode 1/2; 4 → Panel mode 1/3.

An additional actuator rod was manufactured that can be mounted by means of a cap nut. Due to the fact that no free flutter will occur during the tests, aerodynamic loads were not crucial in the design process. Nevertheless, based on potential flow theory calculations, the panel properties are chosen in such a way that in case of a disconnection between the actuator and the panel free flutter will not occur. A strength calculation by means of finite elements methods ensured that the actuator is not able to destroy the panel. In order to implement different deflection shapes the rack provides slots for different actuator configurations. From one cylinder, attached in the middle of the panel, up to three actuators can be placed in the rack. Every configuration establishes another mode shape of the flat plate (Fig. 4).

Mounting Structure

The panel assembly, which is the panel within its massive frame, is bolt mounted to another support structure that is to be integrated into the wind tunnel wall (Fig. 5.). For mounting the panel at the wind tunnel a segment of the tunnel wall (Fig. 6.) was removed and replaced by the test setup. For future experiments the slot where the panel fits in may be used easily for different kinds of panels or other models. A feature of the frame structure is dedicated to the panel's aspect ratio. For a change between test runs the support consists of an outer frame carrying an inner frame, which can be rotated by $\alpha = 90°$ (Fig. 5.). The inner frame carries the panel assembly as well as the actuator rack. The outer frame connects the whole setup with the wind tunnel wall by bolt connections. Both the inner and the outer frame are welded of flat bar steel. Due to the numerous subassemblies, an accurate positioning of the setup is essential. First, the panel assembly and the inner frame with its wall plates have to be flush to the wind tunnel wall because recesses or heels shall not influence the flow. For this purpose thin steel tape is lined between panel assembly and support structure. Ejector screws rearwards the support's wall plates adjust them to the wind tunnel wall (z-direction). Second, the gaps between tunnel wall and model and between the single parts of the model have to be small. Steel angles are mounted at the outer frame sides to adjust the setup in x- and y-direction. The setup can be adjusted with respect to the wind tunnel and the inner frame can be adjusted with respect to the outer frame. While a test is running the panel shall oscillate only with the intended excitation frequency and without secondary frequencies. A basic requirement is that excitation frequencies and natural frequencies of the test setup and the wind tunnel shall not overlap. Several FE aided refinement steps were done until a sufficient safety margin was reached. To some extend the resulting additional strutting is recognizable in Fig. 5.

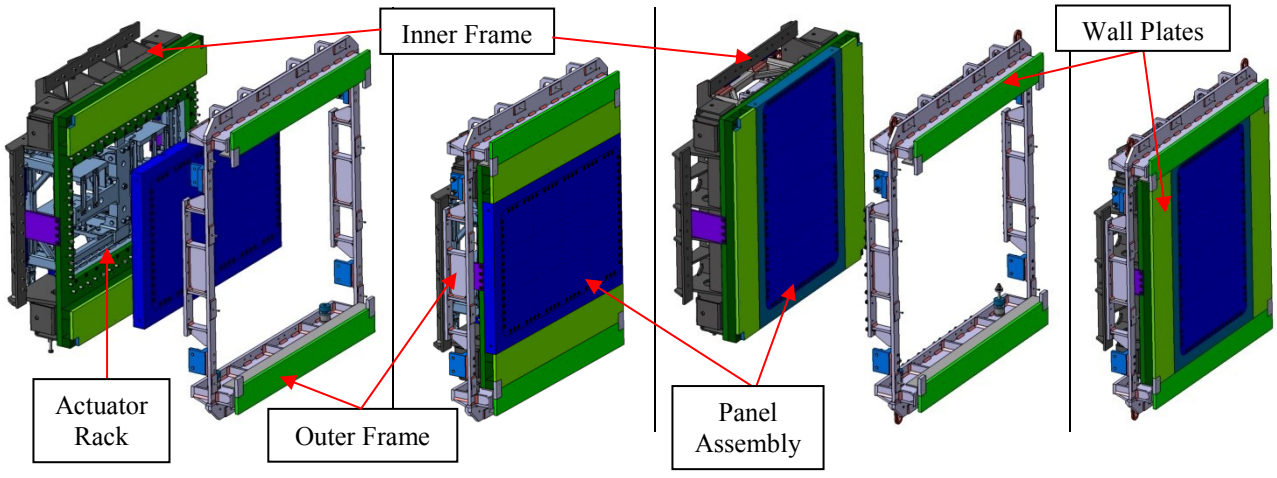

Fig. 5. Panel flutter test setup. (a) Exploded assembly drawing, (b) Setup configuration $\alpha_0 = 0°$, (c) & (d) Setup configuration $\alpha_1 = 90°$.

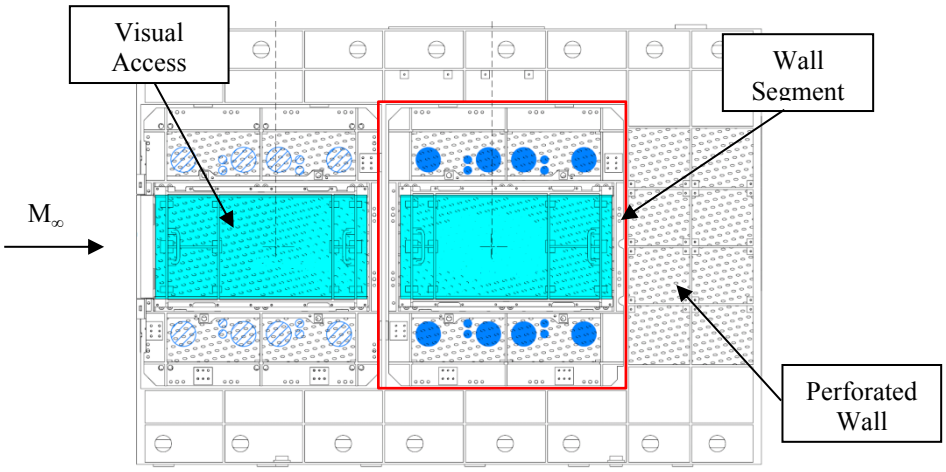

Fig. 6. Front view of the perforated test section east wall.
Two segments on each wall are removable.

Instrumentation

In order to measure the transfer behaviour of the aeroelastic system, measurement techniques for the deformation *dz* and for the pressure *p* are applied. The deformation measurement technique is a stereo camera based marker tracking system, the so-called PicColor system. Two cameras in a certain angle to the perpendicular line of the panel surface and to each other are pointing at markers that are distributed over the panel's surface (Fig. 7.). The cameras are positioned outside the test section behind a window opposite to the panel (Fig. 8.). After a calibration of the system it allows the tracking of the markers by each of the cameras. The two recorded 2D data sets are then computed to one 3D data set by means of a calibration matrix, which was generated before the test run. The frame rate of the tracking process was set f_{Pic} = 450Hz. Crucial for this method of measurement is the achievement of high optical contrasts and frame rates as high as possible. To satisfy the first, white markers are placed on the surface of the dull black panel surface. In addition several spotlights are necessary due to short times of exposure of the cameras. Altogether eighty-two markers were distributed over the panel surface in six lines:

- Stream wise: $y_{dz,1} = 0.33w_i$, $y_{dz,2} = 0.5w_i$, $y_{dz,3} = 0.66w_i$
- Cross stream wise: $x_{dz,1} = 0.3a_i$, $x_{dz,2} = 0.5a_i$, $x_{dz,3} = 0.7a_i$

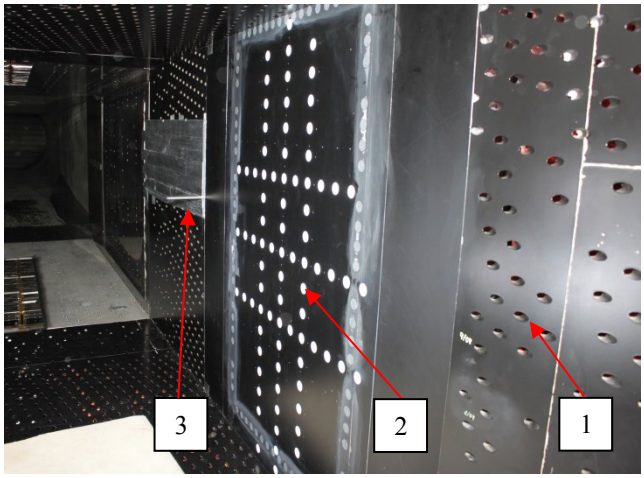

Fig. 7. View in direction of flow. Perforated wall steel sheets (1); Panel with markers (2); Boundary layer rake (3).

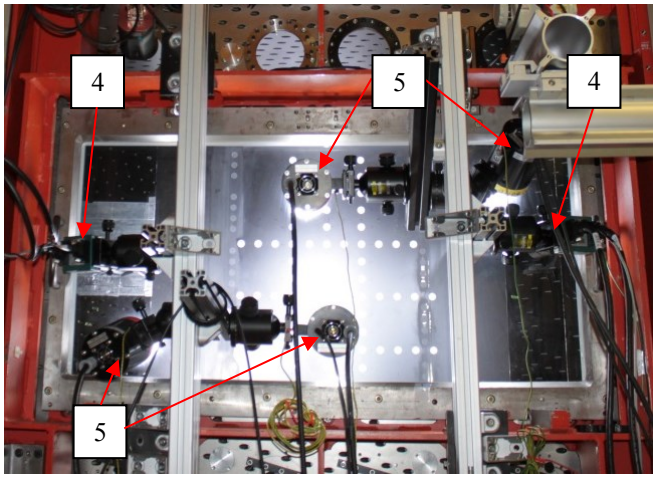

Fig. 8. View from outside the test section at the panel through a window. The aluminium rack carries cameras (4) and spot lights (5).

In quite a similar way 108 unsteady pressure transducers (Kulite-XCS-093) are distributed in another six lines (Fig. 2.):

- Stream wise: $y_{cp,1} = 0.25w_i$, $y_{cp,2} = 0.5w_i$, $y_{cp,3} = 0.75w_i$
- Cross stream wise: $x_{cp,1} = 0.25a_i$, $x_{cp,2} = 0.5a_i$, $x_{cp,3} = 0.75a_i$

Those transducers show a pressure range of 0.35bar and an acceleration sensitivity (transversal) of $2.2 \cdot 10^{-4}$% of the full scale output (FSO). Each transducer is put in a plastics carrier, which is a small tube bend in an angle of 90 degrees in order to arrange its effective direction transversal to the generated acceleration force (Fig. 9.). Each carrier is adhered in a step hole. Furthermore, the short distances between sensor and panel surface lead to a small enclosed volume, which may have a negligible influence on the measurements. In contrast to the deformation measurement the sampling rate here depends on the excitation frequency of the actuator. Every oscillation period is sampled with a resolution of 128 samples. In Fig. 7. a rake for the measurement of the boundary layer thickness is applied right behind the panel. It consists of 64 Pitot Tubes which are distributed over a height of 100 mm.

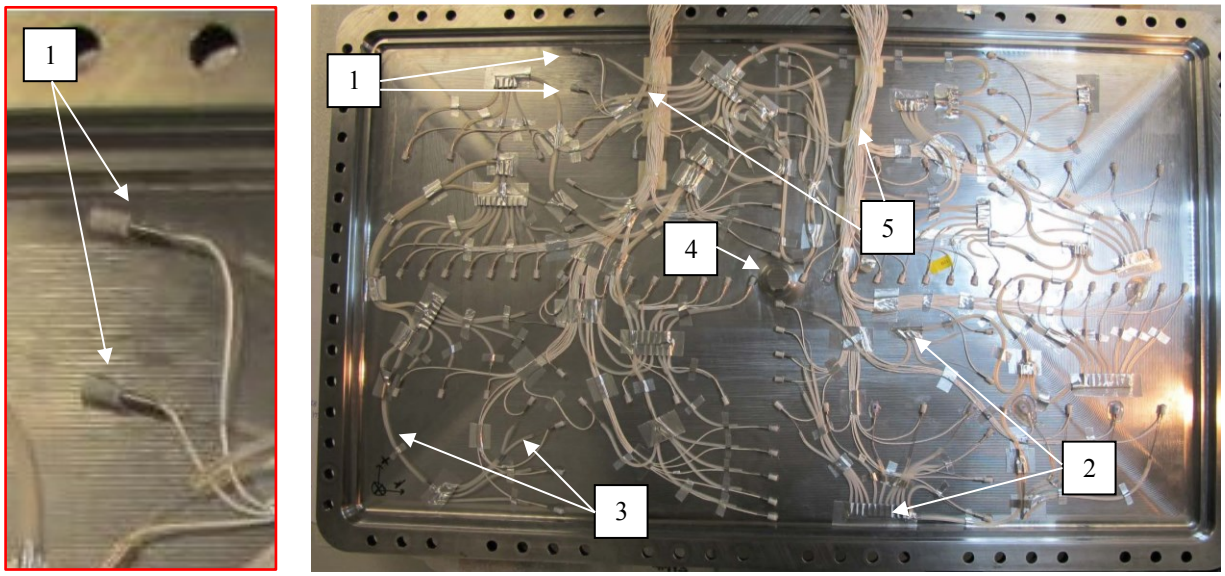

Fig. 9. Rear view of the equipped panel. (1) → Pressure transducers in sensor carriers; (2) → Divider tubes; (3) → Reference pressure tubes; (4) → Actuator connection; (5) → Cable bundles.

Wind Tunnel

The DNW-TWG is a closed return type wind tunnel, which allows experiments in a wide range of Mach numbers. Three test sections, each dedicated for another Mach domain, are available. Tests within the transonic regime are possible by using the so-called perforated test section ($0.3 < M_\infty < 1.2$). The test section has a cross section of 1m by 1m. A pressure chamber, which is surrounding the test section allows a variation of the total pressure in a range within approximately $35\text{kPa} < p_0 < 135\text{kPa}$. The measurement points of the conducted experiments within the total operation range are illustrated in Fig. 10. The dark green bars indicate the Mach number ranges which the three different test sections are dedicated to. The test section shows four possibilities to exchange wall segments (wall surface 1m by 1m) and replace them with different kinds of models.

Test Procedure

The Mach number range ($0.7 < M_\infty < 1.2$) was divided into steps of $\Delta M_\infty = 0.05$ for a proper resolution. The total pressure level varied within $0.3\text{bar} < p_0 < 0.4\text{bar}$, what leads to a low level of aerodynamic loads interacting with the panel. The Reynolds number was constant at Re = 2.5E+06

based on the reference length a_i. Once constant flow conditions had been reached, the parameters chosen for the panel's first mode motion were varied. Here, the frequency f and the amplitude $\hat{A}$ of the panel's center deflection were varied within a range of f_{min} = 0.0Hz and f_{max} = 105.0Hz (Δf = 7.5Hz) for three distinct amplitudes $\hat{A}_1$ = 0.6mm, $\hat{A}_2$ = 1.2mm and $\hat{A}_3$ = 1.8mm. Flow parameters and model parameters are shown in table 1 and table 2. The reduced frequency ω^* is calculated by Eq. 4.

$$\omega^* = \frac{2\pi f}{c_\infty} \tag{4}$$

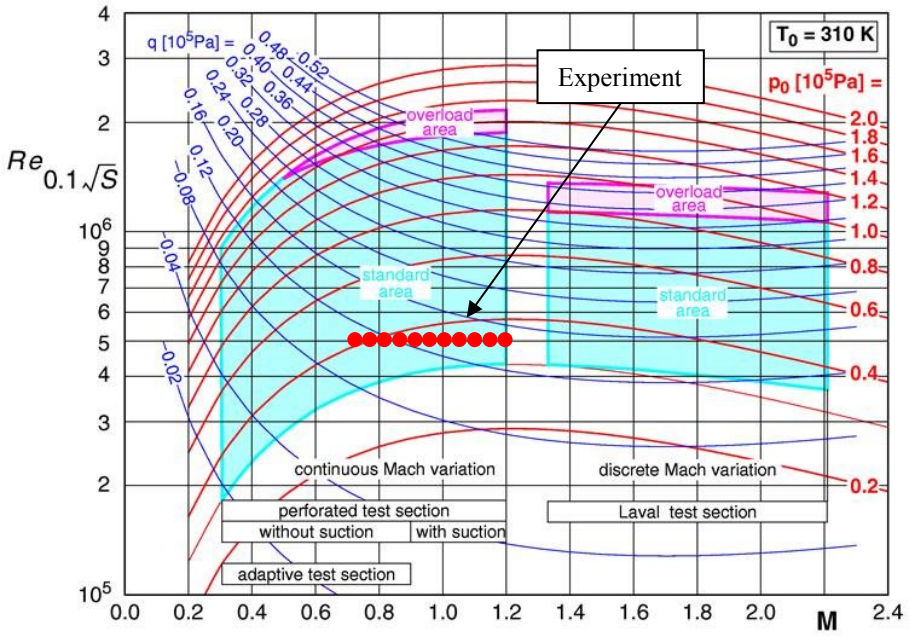

Fig. 10. Operation range of the DNW-TWG. Reynolds number (reference length l_{Re} = 0,1m) vs. Mach number is plotted with the corresponding total pressure and dynamic pressure.

Table 1. Flow Parameters.

Parameter	Min	Max
M_∞ [-]	0.7	1.2
p_0 [kPa]	34.8	42.0

Table 2. Model Parameters.

Parameter	Min	Max
ω^* [-]	0.0	1.4
f [Hz]	0.0	105.0
$\hat{A}$ [mm]	0.6	1.8

3. RESULTS

In this section the focus is laid onto the accuracy of the panel motion forced by the actuator and onto the flow response presented by the measured pressures. The measurement points considered in the following analysis are presented in table 3. The lower Mach number is also the lowest Mach number of the conducted experiments. The second Mach number is the highest that was reached in the experiments. For each Mach number one frequency of the low spectrum and one of the mid spectrum is chosen (the interpretation of the high spectrum oscillation is still in progress). The regarded amplitude is $\hat{A}_3$, though the other two amplitudes are used as well for comparison in the last part of this section (Table 3). The hydraulics purpose is the deflection of the panel center with certain amplitudes and frequencies. To estimate the gained accuracy of the latter Fast Fourier Transformations are shown in Fig. 11. for the regarded cases. The amplitude is plotted versus the frequency spectrum in which the signal of the actuator and the signal of the PicColor (marker in the panel center) measurements are compared. The amplitude is made nondimensional by dividing with

$\hat{A}_3$. That the intended oscillation is transmitted to the actuator and finally to the panel center can be seen at the global peaks (amplitude of 10^0) which are located where the intended excitation frequency (red dashed line) is depicted.

Table 3. Analyzed measurement points.

M_∞ [-]	f [1/s]	$\hat{A}_3$ [mm]	$\hat{A}_2$ [mm]	$\hat{A}_1$ [mm]
0.7	1.0	1.8	1.2	0.6
	45.0	1.8	1.2	0.6
1.2	1.0	1.8	1.2	0.6
	37.5	1.8	1.2	0.6

Beside those peaks several local peaks in the actuator signal are depicted at amplitudes in order of about 10^{-4}, which are recognizable in the PicColor signal as well (order of 10^{-2}). Those oscillations are owed to the frequency generator output which shows multiples of the adjusted frequency. In addition, a lot of noise at low amplitudes is shown for the actuator signal and the PicColor signal at an order of magnitude of 10^{-5} and 10^{-3}, respectively. Here, the impact of the wind tunnel compressor and auxiliary systems are influencing factors.

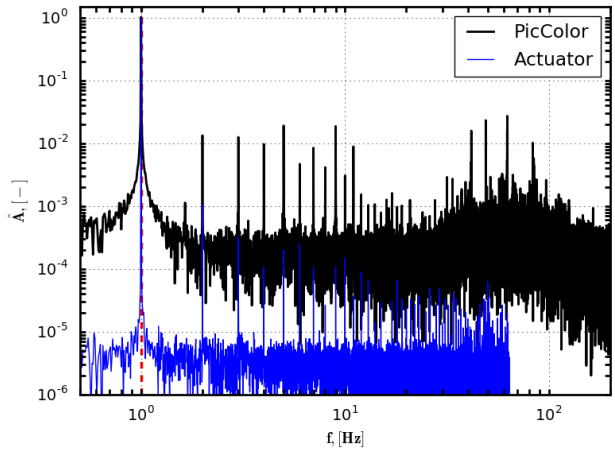

(a) $M_\infty = 0.7$, $f = 1.0$Hz, $\hat{A}_3 = 1.8$mm

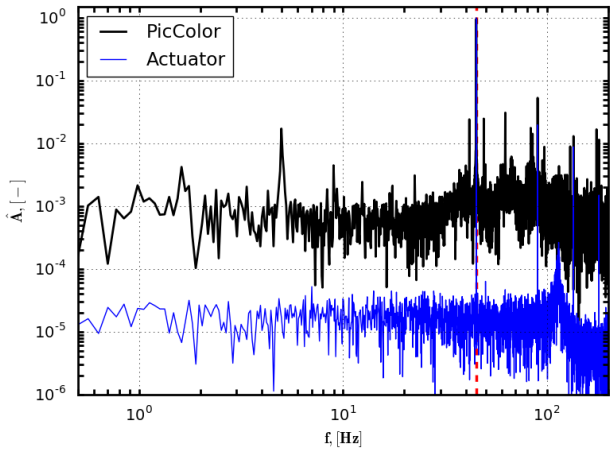

(b) $M_\infty = 0.7$, $f = 45.0$Hz, $\hat{A}_3 = 1.8$mm

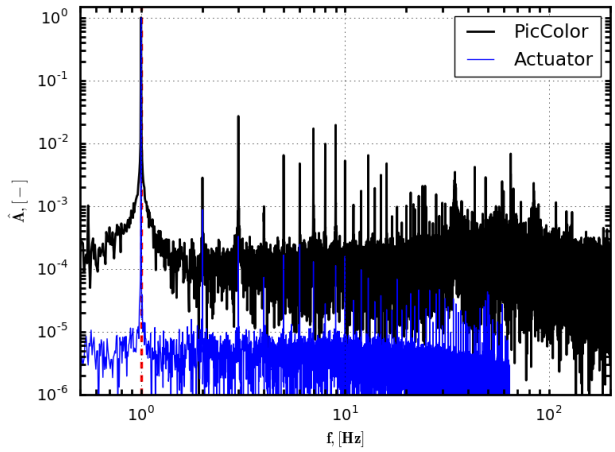

(c) $M_\infty = 1.2$, $f = 1.0$Hz, $\hat{A}_3 = 1.8$mm

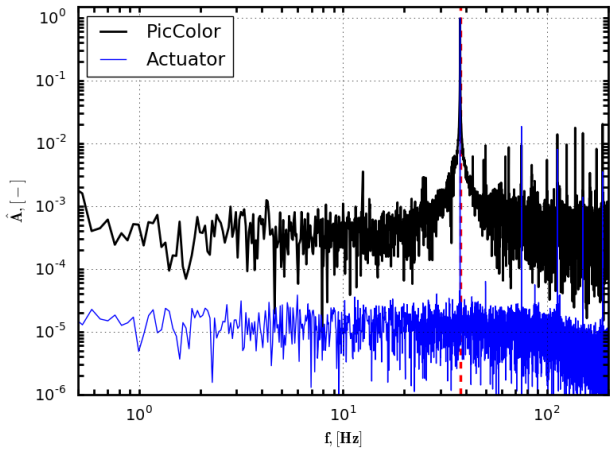

(d) $M_\infty = 1.2$, $f = 35.0$Hz, $\hat{A}_3 = 1.8$mm

Fig. 11. Fast Fourier Transformation of the panel center deflection.

Next the amplitude and the panel shape are to be verified. What is rudimental shown in Fig. 11. is depicted more exact in Figs. 12-15. Those figures show deflections as well as c_p-values for all six PicColor and pressure transducer sections for the point in a period, where the panel deflection has its maximum. The measured pressure is shown in the two top subfigures, of which the left one shows results of the streamwise sections and the right one those of the cross streamwise measurements. The pressure coefficient amplitude is normalized by the deflection amplitude. The subfigures below present the panel deflection in the same way the top figures present the pressure coefficient. In addition an analytical function of the ideal deformation is illustrated (dashed line), which is only displayed for the panel center lines. The deflection is normalized by division by the nominal deflection amplitude. In the case of the streamwise deflection in Fig. 12. the deflection of each point is in a good agreement with the ideal function. The same statement is valid for the high Mach number with low frequency excitation in Fig. 14. In cross streamwise direction the amplitude matches also well the intended value. The shape however shows discrepancies. This may be due to the fact, that the panel width (cross streamwise) has almost twice the distance of the panel length. The connection of the actuator takes an area in the center of the panel. There, the panel is forced in a horizontal position. This impact is for the short distance stronger than for the long one. In case of the latter, the structure shape is able to bend downward where the other is still forced into the horizontal shape. The same phenomenon can be observed in all four illustrated examples. Measurements at high excitation frequency are presented in Fig. 13. and Fig. 15. For both cases the actual amplitude is only close to the intended one. A slight decrease in amplitude of the actuator at higher frequencies was observed as well. In all regarded cases a good symmetrical behavior with respect to the panel center lines was observed. During the tests the wind tunnel is subdued to a slight heating mainly induced by the operation of the tunnel engine. This may have an influence on the panel deformation shape as it may cause bumps due to the panel lengthening. Another parameter to consider is the influence of the volume at the panel surface which is not exposed to the flow, though an actual enclosed volume is not present here. Neither an influence of the temperature input nor of the gas volume behind the panel is recognized.

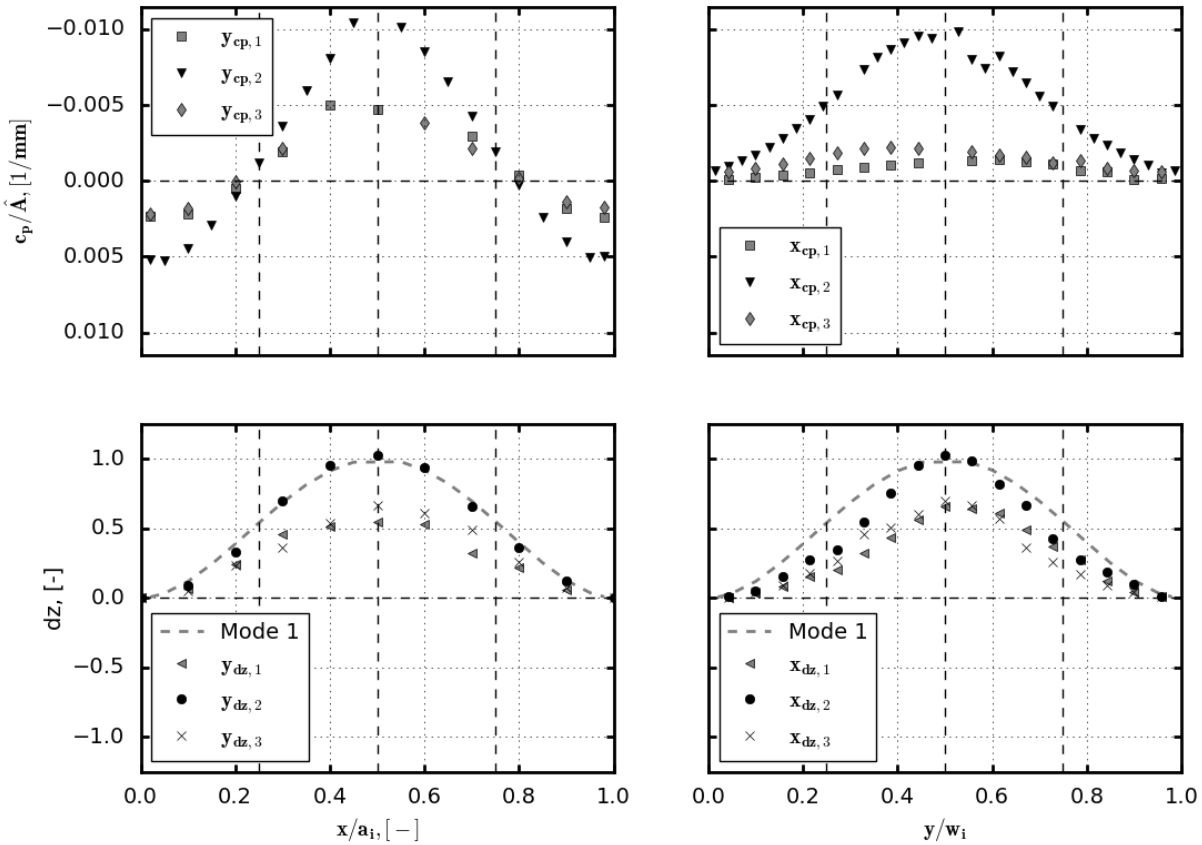

Fig. 12. Pressure coefficient and deflection at $M_\infty = 0.7, f = 1.0\text{Hz}, \hat{A}_3 = 1.8\text{mm}$.

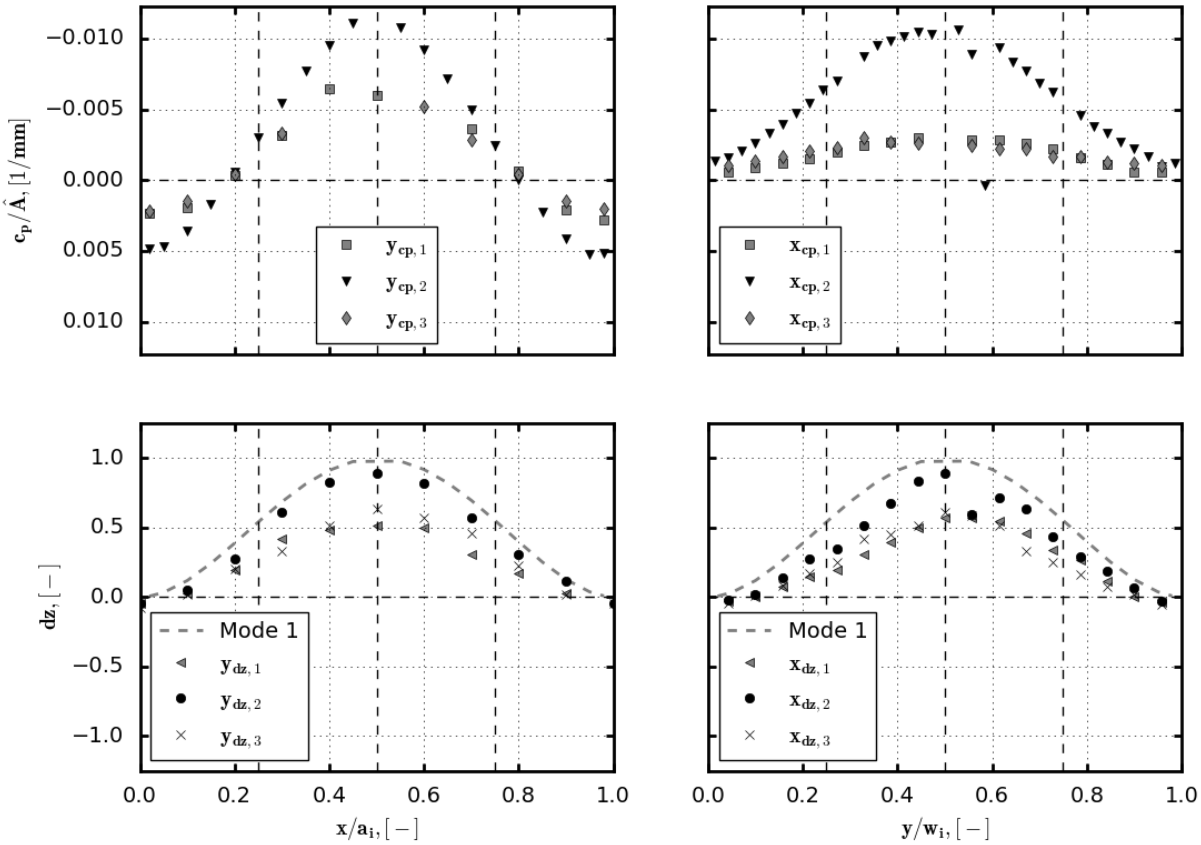

Fig. 13. Pressure coefficient and deflection at $M_\infty = 0.7, f = 45.0\text{Hz}, \hat{A}_3 = 1.8\text{mm}$.

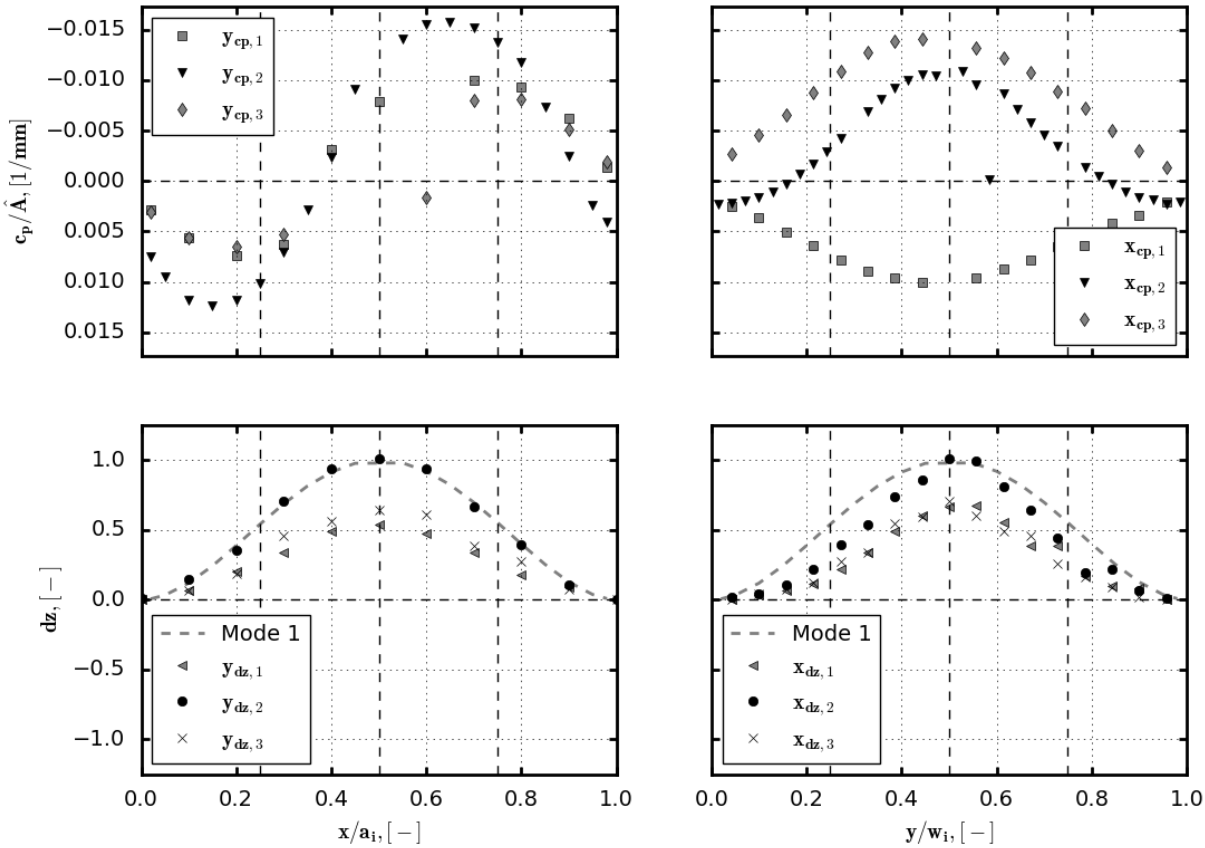

Fig. 14. Pressure coefficient and deflection at $M_\infty = 1.2, f = 1.0\text{Hz}, \hat{A}_3 = 1.8\text{mm}$.

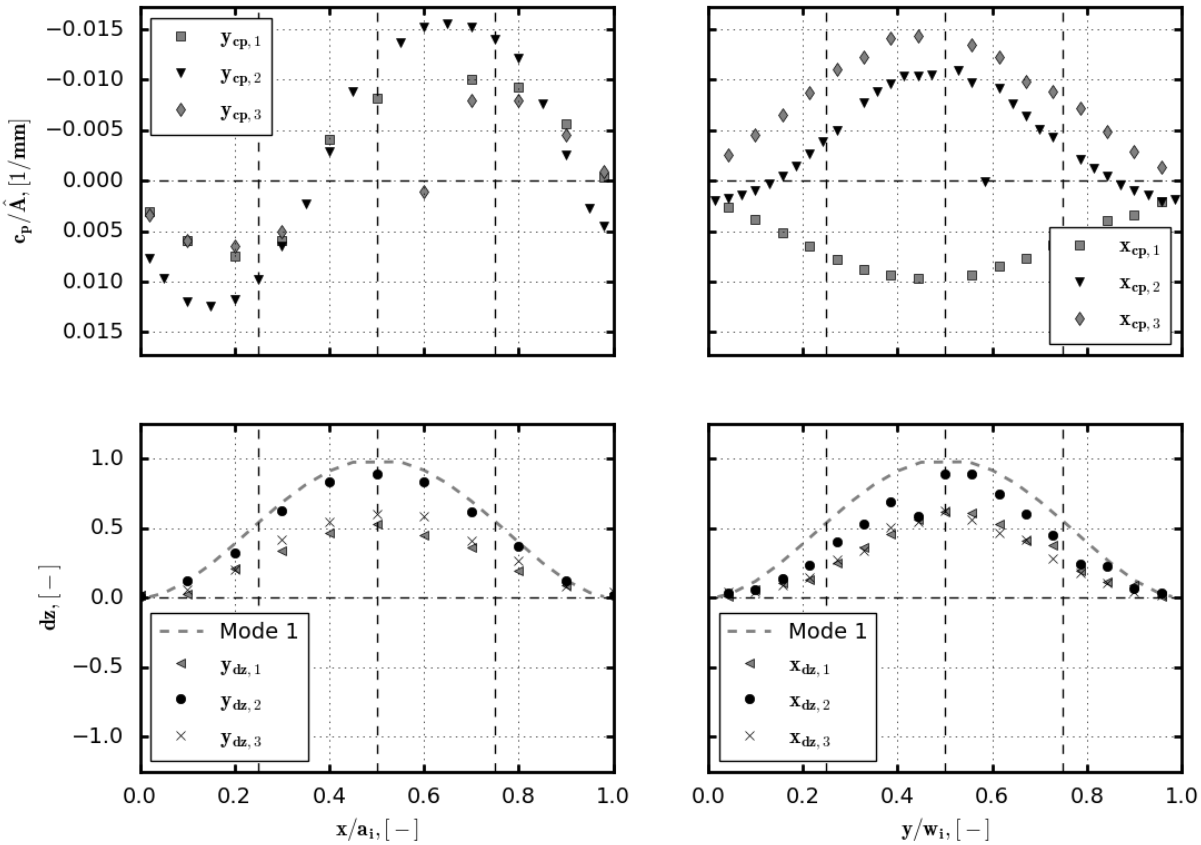

Fig. 15. Pressure coefficient and deflection at $M_\infty = 1.2, f = 35.0\text{Hz}, \hat{A}_3 = 1.8\text{mm}$.

The prior presented measurements were limited to nominal amplitudes of $\hat{A}_3 = 1.8$ mm, which is only one of three tested amplitudes. The choice of adequate amplitudes is a dilemma because the requirements for the experiment oppose those of the numerical activities. The former needs values as high as possible in order to gain distinct sensor readings. In contrast to that, in order to avoid nonlinearities for all parts of the aeroelastic system, the values have to be as small as possible. With regard to an aeroelastic stability boundary the amplitudes are infinitesimal. A comparison of the three chosen amplitudes is shown in Figs. 16. The attention is drawn to the pressure coefficient, which presents the aerodynamic response of the panel deflection. The upper two graphs in Fig. 16. reveal the pressure coefficients for all amplitudes along the panel length (x-direction, black) and its width (y-direction, red). The values are again divided by the referring nominal amplitudes. A very good agreement of the data for all three amplitudes is found for all cases that leads to the assumption of a linear system in the observed range of amplitudes. Two transducers of each center line (streamwise: no. 7, cross streamwise: no. 14) are chosen to ensure, that the agreement is also valid for one oscillation period (lower subfigures in Fig. 16).

Since it is known that the turbulent boundary layer has an impact on aeroelastic stability its thickness is measured at each test measurement point. Fig 17. illustrates the results. The left figure shows the nondimensional wall distance (z-coordinate) and the nondimensional Mach number. This reveals their resemblance with respect to the profile shape. Two Power Law approaches with different exponents are implemented also to prove the turbulent character. In the right figure the real wall distance and each boundary layer thickness is shown. A dependency on the Mach number is observed, which is unusual since only a dependency on the Reynolds number should occur. Nevertheless, with increasing Mach number the boundary layer thickness decreases from about 6.5 mm to 4.5 mm. Note that the accuracy of the measurements are limited by the rake's resolution. No impact of the excitation frequency on the steady pressure measurements is observed.

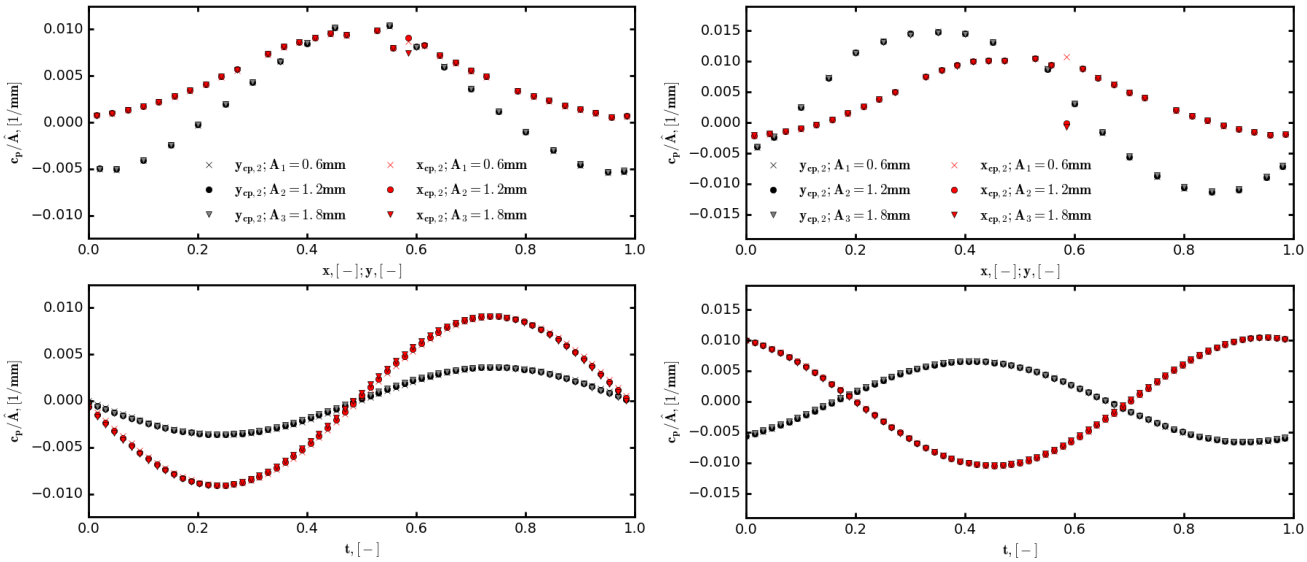

a) $M_\infty = 0.7$ and $f = 1.0$Hz b) $M_\infty = 1.2$ and $f = 37.5$Hz

Fig. 16. Comparison of amplitudes influence on aerodynamic response.

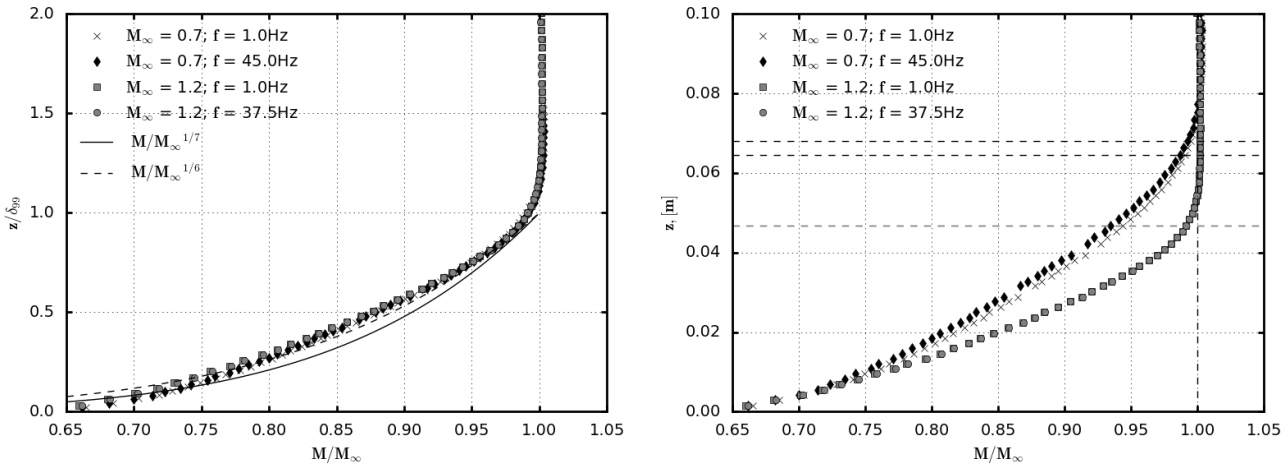

a) Measured boundary layer profiles and theoretical profiles.

b) Measured boundary layer thicknesses.

Fig. 17. Boundary layer measurements.

4. CONCLUSIONS

The design of the new DLR panel flutter test setup was described. An oscillating panel, driven by hydraulics, was investigated in the transonic regime concerning its aeroelastic stability. The shape, which the panel was forced into, was that of a flat plate's first mode. Measurement techniques collected data for deflection and pressure distribution. The initial operation and the discussion of the first results were discussed. Here, amplitude, structure shape excitation frequency and the measured boundary layer thickness were observed.

a. Actual amplitude and intended amplitude are in a good agreement, although a slight decrease in realized amplitude at higher frequencies was noticed.
b. The forced shape, which should be similar to a flat plate mode one shape, was confirmed. Especially the stream wise outline was convincing.

c. The transfer of the aimed frequency range to the panel occurred, even though higher harmonics of the excitation frequency in the spectrum of the actuator signal and increased noise in case of the PicColor deflection measurement system were present.
d. The boundary layer thickness measurements show a dependency on the free stream Mach number. The obtained values are in between 4.5mm < δ_{99} < 6.5mm.

5. OUTLOOK

The presented test was the first experiment of the panel flutter test rig and its initial run. The presented results showed its functional capability. In the next step and based on the data gained for the pressure distribution over the panel and its deformation the energy transfer between flow and panel structure will be investigated.
As indicated by former investigations and the coupled CFD/FEM calculations by the DLR, both the first and the second panel mode shape are to be taken into account for understanding the flutter phenomenon. The manufacturing of another panel, a mode-2 panel, is in progress at the DLR. Its operation in the DNW-TWG is scheduled in winter 2016/2017. The combined data sets will give a detailed base for further stability analysis.

6. ACKNOWLEDGEMENTS

The work presented in the report on hand was done within a cooperation of the DLR Institute of Aeroelasticity, DLR Institute of Aerodynamics and Flow Technology and Airbus DS. Thanks go to Johannes Nuhn and Thomas Büte from the DLR Institute of Aeroelasticity for operating the experiment, to Norbert Kassler and Michael Reuter from the DLR fitter's shop for pressing the setup into the test section by brute force and to all colleagues who were on spot. Additionally thanks go to Bernhard Kotzias and Peter Nöding (Airbus DS) for the support.

7. REFERENCES

[1] Jordan, P. F., *Über das Flattern von Beplankungen*, AVA research report B 45/J/3, 1945.

[2] Jordan, P. F., *The Physical Nature of PANEL FLUTTER*, AERO DIGEST, pp. 34-38, 1956.

[3] Meier, H.-U., *Die deutsche Luftfahrt, Die Pfeilflügelentwicklung in Deutschland bis 1945*, Bernhard & Graefe Verlag, Bonn, pp. 251 , 2006.

[4] Bohon, H. L., *PANEL FLUTTER TESTS ON FULL-SCALE X-15 LOWER VERTICAL STABILIZER AT MACH NUMBER OF 3.0,* NASA Technical Note D-1385, 1962.

[5] Lall, T. R., INTERSTAGE ADAPTER PANEL FLUTTER ON ATLAS-CENTAUR AC-2. AC-3 AND AC-4 VEHICLES, NASA Technical Memorandum X-1179, 1965.

[6] Muhlstein, L., Gaspers, P. A., Riddle, D.W., *An experimental study of the influence of the turbulent boundary layer on panel flutter*, NASA Technical Note D-4486, 1968.

[7] Muhlstein, L., *A FORCED VIBRATION TECHNIQUE FOR INVESTIGATION OF PANEL FLUTTER*, AIAA Paper, No, 66-769, AIAA Aerodynamic Testing Conference, 1966.

[8] Gaspers, P. A., Muhlstein, L., Petroff, D. N., *Further experimental results on the influence of the turbulent boundary layer on panel flutter*, NASA technical note D.Bd.5798, 1970.

[9] Lock, M. H., Fung, Y. C., *Comparative experimental and theoretical studies of the flutter of flat panels in a low supersonic flow*, Technical report, California Institute of Technology, Pasadena, 1961.

[10] Vedeneev, V. V., Guvernyuk, S. V., Zubkov, A. F., Kolotnikov, M. E., *Experimental Observation of Single-Mode Panel Flutter in a Supersonic Gas Flow*, Doklady Akademii Nauk, Vol. 427, No. 6, pp. 768-770, 2009.

[11] Sylvester, M. A., Baker, E.J., *Some experimental studies of panel flutter at mach number 1.3*, Technical report, National Advisory Committee for Aeronautics (NACA), 1957

[12] Anderson, W., J., *Experiments on the flutter of flat and slightly curved panels at Mach number 2.81*, GALCIT Structural Dynamics Report SM 62-34, California Institute of Technology, 1962.

[13] Ganapathi, M., Varadan, T. K., *Supersonic Flutter of Laminated Curved Panels*, Defense Science Journal, Vol. 45, No. 2, pp. 147-159, 1995.

[14] Dowell, E. H., Voss, H. M., *Theoretical and experimental panel flutter studies in the Mach number range of 1.0 to 5.0*, Defense Technical Information Center, 1965.

[15] Xue, D. Y., Mei, C., *Finite Element Nonlinear Panel Flutter with Arbitrary Temperatures in Supersonic Flow*, AIAA Journal, Vol.31, No., pp. 154-162, 1993.

[16] Dowell, E. H., *Aeroelasticity of Plates and Shells*, Noordhoff International, Leyden, The Netherlands, pp.139 ,1975.

[17] Bohon, H. L., Anderson, M. S., Heard, W. L., *FLUTTER DESIGN OF STIFFENED-SKIN PANEL FOR HYPERSONIC AIRCRAFT*, NASA TECHNICAL NOTE, NASA TN D-5555, 1969.

[18] Kouchakzadeh, M. A., Rasekh, M., Haddadpour, H., *it Panel flutter analysis of general laminated composite plates*, Composite Structures 92, 2010.

[19] Shiau, L. C., Lu, L. T., *Nonlinear Fltter of Two-Dimensional Simply Supported Symmetric Composite Laminated Plates*. Journal of Aircraft, Vol. 29, No. 1, pp. 140-145, 1992.

[20] Dixon, I. R., Mei, C., *Finite Element Analysis of large-Amplitude Panel Flutter of Thin Laminates*. AIAA Journal, Vol.31, No.4, 1993.

[21] Ashley, H., Zartarian, G., *Piston Theory: A New Aerodynamic Tool for the Aeroelastician*, Journal of the Aeronautical Sciences, Vol. 23, No. 12, pp. 1109-1118, 1956.

[22] Hashimoto, A., Aoyama, T., and Nakamura, Y., *Effects on Turbulent Boundary Layer on Panel Flutter*, AIAA Journal, Vol.47, No.12, pp. 2785-2791, 2009.

[23] Alder, M., *Development and Validation of a Partitioned Fluid-Structure Solver for Transonic Panel Flutter with Focus on Boundary Layer Effects*, AIAA Journal, Vol. 53, No. 12, pp. 3509-3521, 2015.